BIOCHEMISTRY
including biophysical chemistry & molecular biology

Article

pubs.acs.org/biochemistry

The Membrane Modulates Internal Proton Transfer in Cytochrome *c* Oxidase

Linda Näsvik Öjemyr,[†] Christoph von Ballmoos,[†] Kristina Faxén,[†,‡] Emelie Svahn,[†] and Peter Brzezinski*[,†]

[†]Department of Biochemistry and Biophysics, The Arrhenius Laboratories for Natural Sciences, Stockholm University, SE-106 91 Stockholm, Sweden

[‡]Department of Plant Biology and Biotechnology, Faculty of Life Sciences, University of Copenhagen, DK-1870 Frederiksbjerg C, Denmark

ABSTRACT: The functionality of membrane proteins is often modulated by the surrounding membrane. Here, we investigated the effect of membrane reconstitution of purified cytochrome *c* oxidase (Cyt*c*O) on the kinetics and thermodynamics of internal electron and proton-transfer reactions during O_2 reduction. Reconstitution of the detergent-solubilized enzyme in small unilamellar soybean phosphatidylcholine vesicles resulted in a lowering of the pK_a in the pH dependence profile of the proton-uptake rate. This pK_a change resulted in decreased proton-uptake rates in the pH range of ∼6.5−9.5, which is explained in terms of lowering of the pK_a of an internal proton donor within Cyt*c*O. At pH 7.5, the rate decreased to the same extent when vesicles were prepared from the pure zwitterionic lipid 1,2-dioleoyl-*sn*-glycero-3-phosphocholine (DOPC) or the anionic lipid 1,2-dioleoyl-*sn*-glycero-3-phospho(1-*rac*-glycerol) (DOPG). In addition, a small change in the internal Cu_A−heme *a* electron equilibrium constant was observed. This effect was lipid-dependent and explained in terms of a lower electrostatic potential within the membrane-spanning part of the protein with the anionic DOPG lipids than with the zwitterionic DOPC lipids. In conclusion, the data show that the membrane significantly modulates internal charge-transfer reactions and thereby the function of the membrane-bound enzyme.

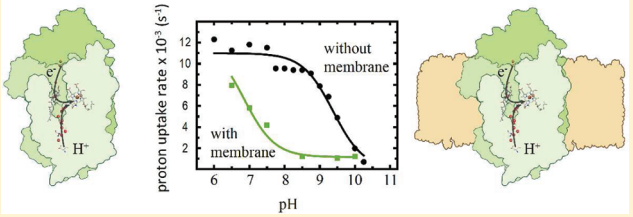

The heme-copper oxidases are membrane-bound enzymes, which catalyze reduction of oxygen to water in the respiratory chain of aerobic organisms. In the cytochrome *c* oxidases (Cyt*c*Os), electrons are transferred one by one from cytochrome *c*, which binds at the more positive (*p*) side of the membrane. The initial electron acceptor in Cyt*c*O is a copper site, Cu_A, from which electrons are then transferred consecutively to a heme group, heme *a*, and to the catalytic site, which consists of heme a_3 and Cu_B. In the bacterial Cyt*c*Os studied to date, protons are transferred through one or two pathways, which start at the more negative (*n*) side of the membrane (for reviews of the structure and function of Cyt*c*Os, see, for example, refs 1−7). Because electrons and protons are transferred from opposite sides of the membrane, this process results in a charge separation across the membrane, which conserves part of the free energy available from the O_2-reduction process. In addition, the reaction is also linked to proton pumping from the *n* side to the *p* side, across the membrane, thereby increasing the overall energy conservation efficiency to two translocated charges per electron transferred to O_2.

In the *Rhodobacter sphaeroides* Cyt*c*O (aa_3 oxidase), two proton pathways have been shown to be used for proton uptake from the *n* side of the membrane[1,5,8] (Figure 1A). Upon reduction of heme a_3 and Cu_B, two protons are transferred through the K pathway, which spans the distance from $Glu101^{II}$ in subunit II (the superscript indicates the subunit number) to the catalytic site in subunit I, via a highly conserved Lys362 residue. After O_2 binds to heme a_3, the two remaining protons are taken up through another proton pathway denoted by the letter D after a conserved Asp132 residue located at the orifice of the pathway. This pathway leads via a highly conserved Glu286 residue to the catalytic site as shown in Figure 1A.[9,10] All protons that are pumped by the Cyt*c*O are also taken up through the same, D pathway, but the trajectory of these protons leads from Glu286 to an acceptor site that is located above the hemes.

Most functional studies of Cyt*c*O to date have been performed with the detergent-solubilized Cyt*c*O. The results from these studies have provided information about rates of internal electron- and proton-transfer reactions as well as pK_a values of internal proton donors. However, understanding the function of a membrane-bound protein such as Cyt*c*O requires studies of reactions catalyzed by Cyt*c*O also in a membrane environment, which would mimic the natural environment of this protein. For example, early measurements of Cyt*c*O turnover showed that the reaction is modulated by the lipid composition.[11] More recent crystallographic and functional

Received: December 7, 2011
Revised: January 16, 2012
Published: January 17, 2012

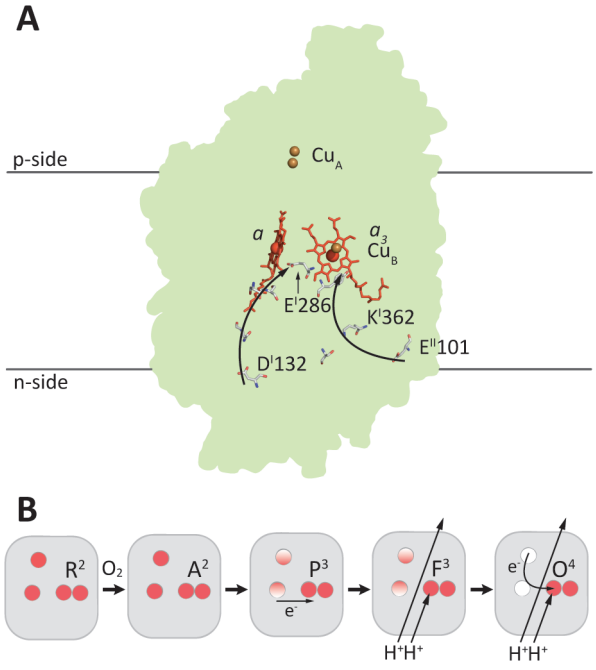

Figure 1. (A) Schematic view of the structure of the *R. sphaeroides* CytcO (Protein Data Bank entry 1M56[9]) embedded in a membrane. The redox-active metal sites and some amino acid residues lining the two proton-transfer pathways are shown, and those mentioned in the text are indicated. (B) Reaction of the fully reduced CytcO with O_2. Red and white circles denote the reduced and oxidized metal centers, respectively (when partly red, the site is partly reduced). The one-letter codes denote the state of the catalytic site with the number of electrons residing at the catalytic site as a superscript. When the CytcO is fully reduced, the catalytic site harbors two electrons (state R^2). After O_2 binds to the reduced heme a_3 (forming state A^2), the O–O bond is broken, associated with transfer of an electron from heme *a* to the catalytic site forming the P^3 state. During the subsequent $P^3 \rightarrow F^3$ reaction, a proton is transferred to the catalytic site, and there is a fractional electron transfer from Cu_A to heme *a* over the same time scale. The forth electron is then simultaneously transferred to the catalytic site with uptake of a proton to the catalytic site forming the O^4 state. In addition, one proton at a time is translocated across the membrane during $P^3 \rightarrow F^3$ and $F^3 \rightarrow O^4$ reactions.

studies have revealed a number of functionally important, specific lipid–CytcO interactions and lipid-binding sites in CytcO. In addition, there are numerous reports of functional modulation of other integral membrane proteins by the surrounding lipid bilayers.[10,12−20] An example of a highly specific protein–membrane interaction in CytcO was demonstrated in a recent study, which showed that the uptake of protons through the K pathway was accelerated by a factor of almost 10 upon reconstitution of the CytcO into a membrane.[21−23] In this case, the effect was attributed to interactions between the lipid headgroups and a protonatable site at the proton pathway orifice, which is located very close to the protein–membrane interface.[22]

In this study, we examine the O_2-reduction reaction in *R. sphaeroides* CytcO reconstituted into membranes. In this reaction, proton uptake takes place through the D pathway, which has an entry point that is located >10 Å from the nearest protein–membrane interface. We used an experimental approach called the flow-flash technique in which the CytcO is first reduced by four electrons residing at each of the redox sites and a blocking CO ligand is bound at heme a_3. The CO–CytcO complex is rapidly mixed with a solution containing O_2, after which the CO ligand is dissociated by means of a short laser flash, allowing O_2 to bind to heme a_3 (the reaction is summarized briefly in Figure 1B) (for reviews, see refs 4 and 24). The state in which heme a_3 and Cu_B are reduced and O_2 is bound to heme a_3 is denoted A^2, where the superscript reflects the number of electrons residing at the catalytic site. Results from numerous earlier studies, primarily with the detergent-solubilized CytcO, have shown that after O_2 binds to the *R. sphaeroides* CytcO an electron is transferred from heme *a* to the catalytic site with a time constant of ~50 μs, which is associated with breaking of the O–O bond and formation of a state called peroxy, P^3. This reaction is followed in time by the uptake of two protons through the D pathway with a time constant of ~100 μs, one that is pumped across the membrane to the *p* side and one to the catalytic site to form a ferryl state, F^3. On the same time scale, there is also a fractional electron transfer from Cu_A to heme *a* that yields ~50% oxidation of Cu_A. Finally, the electron from the Cu_A–heme *a* equilibrium is transferred to the catalytic site, forming the oxidized state O^4, with a time constant of ~1 ms, linked to uptake of two protons through the D pathway as described for the $P^3 \rightarrow F^3$ reaction described above.

Here, we investigated the pH dependence of the reaction with O_2 of reduced CytcO, reconstituted in membranes with different lipid compositions. The results show that both the proton-transfer rates and electron equilibria were modulated upon reconstitution into the membrane.

MATERIALS AND METHODS

Growth of Bacteria and Purification of Cytochrome *c* Oxidase. *R. sphaeroides* was grown in Sistrom medium, and His-tagged CytcO was purified with affinity chromatography using a Ni-NTA column as described previously.[25] After elution, the buffer was exchanged into 100 mM HEPES (pH 7.4) containing 0.1% *n*-dodecyl β-D-maltoside (DDM, Glycon, Germany) before being frozen in liquid nitrogen. The purified enzyme was stored at −80 °C until it was used.

His-tagged *Thermus thermophilus* ba_3 CytcO was expressed and purified as described previously[26] with the following modifications. The enzyme was prepared in the presence of 2% Triton X-100 overnight at 4 °C. The membrane extract was then bound to a 5 mL precast Ni-NTA column (His Prep HP, Amersham Biosciences) in the presence of 10 mM imidazole. Washing and elution of the ba_3 oxidase bound to the column were performed in the presence of 50 and 200 mM imidazole, respectively.

Reconstitution of Cytochrome *c* Oxidase in Vesicles with Different Lipid Compositions. A lipid extract from soybean phosphatidylcholine (type II, Sigma) was made by diethyl ether extraction and acetone precipitation. Pure 1,2-dioleoyl-*sn*-glycero-3-phospho-(1′-*rac*-glycerol) (DOPG) and 1,2-dioleoyl-*sn*-glycero-3-phosphocholine (DOPC) lipids (Avtani Polar Lipids, Alabaster, AL) were dissolved to a concentration of 50 mg/mL in a 2:1 chloroform/methanol mixture. For DOPG and DOPC samples, the solvent was evaporated under a flow of nitrogen forming a dry lipid film. Small unilamellar vesicles (SUVs) with a diameter of 60–70 nm were prepared as described in ref 27. Lipids were dissolved in 100 mM KCl, 25 mM HEPES (pH 7.5), and 100 μM EDTA to a final concentration of 3.9×10^{-5} mol/mL (DOPG and DOPC) or 30 mg/mL (soybean lipids). The vesicles were formed by sonication (Ultrasonic VCX 130, Chemical Instru-

dx.doi.org/10.1021/bi201795c | *Biochemistry* 2012, 51, 1092−1100

ments AB) in 30 s on and off cycles at 50% output energy until the solution was transparent. The solution was then centrifuged for 20 min at 4500*g* to remove particles from the sonicator tip before being mixed with sodium cholate and Cyt*c*O to final concentrations of 1% and 5 μM, respectively. Samples were incubated for 1 h at room temperature before the detergent was removed using a gel filtration column (PD-10, GE Healthcare Bio-Sciences AB, Uppsala, Sweden) equilibrated with same buffer that was used for vesicle preparation. The orientation of the Cyt*c*O in the membrane was determined using an assay in which the Cyt*c*O was first reduced by cytochrome *c*, which reduces only the Cyt*c*Os in which the cytochrome *c*-binding site faces the outside, and then by dithionite, which reduces also the inward-facing population. The orientation was found to be 70−80% with the cytochrome *c*-binding site toward the outside for all lipid compositions. The respiratory control ratio (RCR) was determined as the ratio of the activities in the presence and absence of proton and potassium uncouplers (FCCP and valinomycin). RCR values of 3−6 were obtained for vesicles composed of soybean and DOPC lipids, while DOPG vesicles had a lower RCR of ∼2. Samples were stored at 4 °C overnight.

Reconstitution of Cytochrome *c* Oxidase into Vesicles for pH Dependence Measurements. To obtain tighter vesicles for pH dependence measurements, we used the same protocol that was previously used for measurements with different pH values on the two sides of the membrane.[28] Purified Cyt*c*O (initial concentration of ∼130 μM) was diluted to 4−6 μM in a buffer containing 4% (w/v) cholate, 0.15 M KCl, 25 mM bis-tris propane, 25 mM CAPS, and 50 mM sucrose (pH 7.4). Soybean lipids were extracted as described above. A lipid solution was prepared at a concentration of 40 mg/mL in the same buffer as the Cyt*c*O, except that the concentration of cholate was 2% (w/v). The lipids were then sonicated under an atmosphere of N_2 while being kept on ice, using a tip sonicator (Microson ultrasonic cell disruptor XL, Novakemi AB) at 50% energy output during repetitive cycles of 30 s on and 30 s off at a rate of 2 min/mL. After sonication, the SUVs were centrifuged at 1500*g* for 20 min to remove titanium particles and lipid aggregates. The SUVs containing Cyt*c*O were prepared using a modified version of the protocol described in refs 29 and 30. Briefly, the Cyt*c*O and lipid samples were mixed at a ratio of 1:1, and Cyt*c*O was inserted into the SUVs upon removal of detergent using Bio-Beads SM-2 Adsorbent (Bio-Rad Laboratories) and a PD-10 desalting column (Amersham Pharmacia Biosciences). Then, the pH was adjusted to different specific values. Typically, the SUVs were stored on ice in a refrigerator overnight and used the next day. The orientation of Cyt*c*O in the SUVs was ∼75% cytochrome *c*-binding site to the outside, and they displayed an RCR of ∼10.

Preparation of Fully Reduced CO-Bound Enzyme. The SUVs prepared in different lipids [lipid dependence studies (see above)] had the same buffer on both sides of the membrane [100 mM KCl, 25 mM HEPES (pH 7.5), and 100 μM EDTA]. The samples were transferred to Thunberg cuvettes, and the atmosphere was exchanged for nitrogen before reduction with 2 mM ascorbate and 1 μM PMS as a mediator reducing all Cyt*c*O regardless of orientation. The SUVs used for the pH dependence study contained 150 mM KCl, 25 mM bis-tris propane, 25 mM CAPS, and 50 mM sucrose (inside the SUVs) and 150 mM KCl, 100 mM sucrose, 200 μM bis-tris propane, 100 μM EDTA, 100 μM FCCP, and 10 μM valinomycin (outside the SUVs). The samples were reduced using 2−3 mM ascorbate and 0.5−1 μM hexaammineruthenium(II) chloride. This redox mediator did not enter the SUVs and therefore it reduced only Cyt*c*Os with Cu_A facing outward. When samples were reduced, the atmosphere in the cuvette was exchanged for CO.

Flow-Flash Experiments. A locally modified combined stopped-flow/flash photolysis apparatus was used (Applied Photophysics; see ref 31 for a detailed description). Briefly, the reduced CO-bound enzyme was mixed at a ratio of 1:1 with an oxygen-saturated solution containing 100 mM KCl, 25 mM HEPES (pH 7.5), and 100 μM EDTA or 150 mM KCl, 50 mM bis-tris propane, 50 mM CAPS, and 100 μM EDTA (see above). The reaction was initiated 200−300 ms after the samples had been mixed by a short laser flash (532 nm, Brilliant B, Quantel, 200 mJ), which dissociated the CO ligand. The subsequent reaction with oxygen was monitored at different single wavelengths.

RESULTS

Figure 2 shows absorbance changes after initiation of the reaction of the four-electron-reduced Cyt*c*O reconstituted in lipid vesicles composed of soybean lipids (see Materials and Methods) and in a detergent solution with O_2. At 580 nm in a detergent solution (black traces in Figure 2A), there is first a small decrease in absorbance associated with oxidation of heme *a* upon formation of the P^3 state ($\tau \cong 50$ μs; $A^2 \rightarrow P^3$ reaction). This decrease in absorbance is more pronounced at high pH because at lower pH values it is masked by an increase in absorbance ($\tau \cong 100$ μs at pH 7.5), associated with formation of the F^3 state ($P^3 \rightarrow F^3$ reaction) and the fractional reduction of heme *a*. Finally, the absorbance decreases with a time constant of ∼1 ms (at pH 7.5), associated with the transfer of an electron from the Cu_A−heme *a* equilibrium to the catalytic site and oxidation of the enzyme, i.e., the $F^3 \rightarrow O^4$ reaction.

As mentioned above, with the detergent-solubilized Cyt*c*O at pH 6 and 7.5, the $P^3 \rightarrow F^3$ absorbance increase at 580 nm displays a time constant of ∼100 μs. This reaction becomes gradually slower with an increasing pH (cf. the pH 10 trace in Figure 2A), displaying a pK_a of 9.4 in the pH dependence of the rate (Figure 3A). At very high pH values (see the pH 11 trace in Figure 2A), the rate becomes so slow that the $P^3 \rightarrow F^3$ reaction absorbance increase merges with the absorbance decrease associated with the next step, the $F^3 \rightarrow O^4$ reaction.[32] This scenario explains why the absorbance changes at 580 nm vanish beyond ∼100 μs at this pH.

Upon reconstitution of the Cyt*c*O into SUVs, the increase in absorbance associated with the $P^3 \rightarrow F^3$ reaction was seen only at the lowest pH values (see the pH 6 green trace in Figure 2A). At pH 7.6, this increase in absorbance was seen only as a small lag in the time range of ∼100−300 μs, and at pH 10, it merged fully with the absorbance decrease associated with the $F^3 \rightarrow O^4$ reaction. These data suggest that at a given pH, upon reconstitution into a membrane, the $P^3 \rightarrow F^3$ reaction becomes slower such that the qualitative shape of the curve becomes similar to that observed at a higher pH value in a detergent solution.

Because it was difficult to determine the $P^3 \rightarrow F^3$ rate for the membrane-reconstituted Cyt*c*O from the data at 580 nm alone due to the small amplitude of the $P^3 \rightarrow F^3$ absorbance changes at pH >7.5, we also did measurements at 830 nm where oxidation of Cu_A is monitored (Figure 2B). This oxidation reaction occurs in two steps with time constants corresponding to those of the $P^3 \rightarrow F^3$ and $F^3 \rightarrow O^4$ reactions. Because both

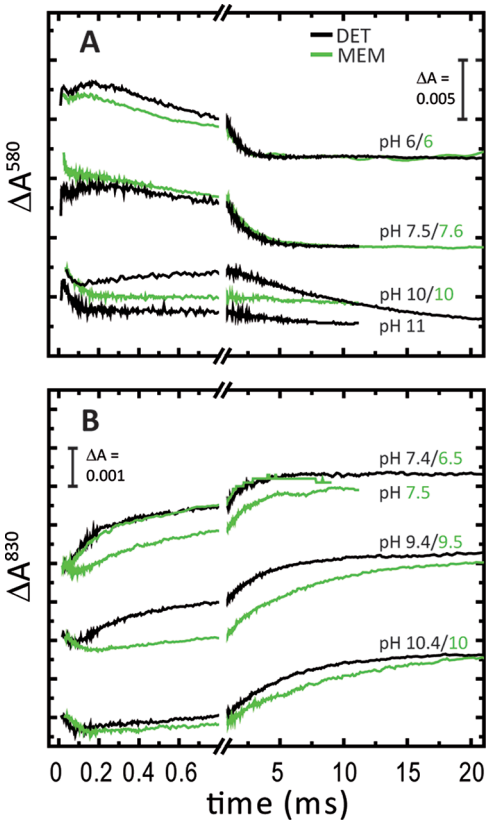

Figure 2. Comparison of absorbance changes upon O_2 reaction with the fully reduced Cyt*c*O at different pH values. (A) In the detergent soluble Cyt*c*O (black, DDM), a rapid decrease in absorbance at 580 nm corresponding to P^3 formation is followed by an absorbance increase and an absorbance decrease due to formation and decay, respectively, of state F^3. For Cyt*c*O reconstituted into soybean vesicles (green, SUV), the absorbance increase corresponding to F^3 formation is seen only at low pH (e.g., pH 6). (B) Oxidation of Cu_A is monitored at 830 nm as an absorbance increase in two kinetic phases that occur over the same time scale as the $P^3 \rightarrow F^3$ and $F^3 \rightarrow O^4$ transitions. The comparison of traces at pH 6.5, 7.4, and 7.5 also highlights the different pH dependence profiles with or without a membrane (see Figure 3). All traces are scaled to 1 μM reacting enzyme. The data with detergent-solubilized Cyt*c*O are from ref 32. In the experiments, vesicles with 150 mM KCl, 25 mM bis-tris propane, 25 mM CAPS, and 50 mM sucrose (inside the SUVs) and 150 mM KCl, 100 mM sucrose, 200 μM bis-tris propane, 100 μM EDTA, 100 μM FCCP, and 10 μM valinomycin (outside the SUVs) were mixed at a 1:1 ratio with an oxygen-saturated buffer containing 150 mM KCl, 50 mM bis-tris propane, 50 mM CAPS, and 100 μM EDTA at different pH values.

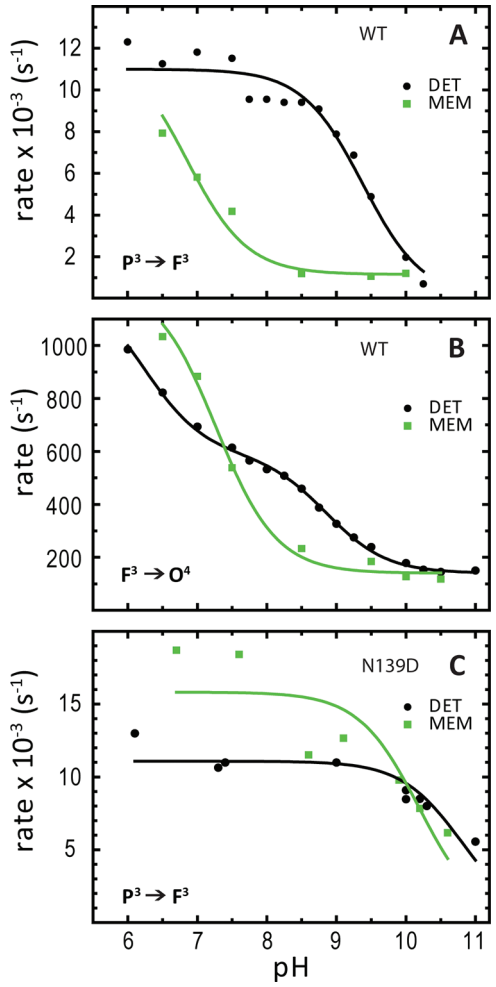

Figure 3. pH dependence of the $P^3 \rightarrow F^3$ (A) and $F^3 \rightarrow O^4$ (B) rates in the wild type and the $P^3 \rightarrow F^3$ reaction with the N139D (C) mutant Cyt*c*O. The rates were determined from 580 nm for detergent-solubilized Cyt*c*O (black dots) or 830 nm for Cyt*c*O reconstituted into soybean vesicles (green squares). The solid lines are fits of data with a pK_a of 9.4 (black line, detergent-solubilized Cyt*c*O) or 6.8 (green line, membrane-reconstituted Cyt*c*O; here we assumed that the rate is saturated at low pH at the same maximal value as with the detergent-solubilized Cyt*c*O). (B) Rates for the $F^3 \rightarrow O^4$ transition as a function of pH. The same color coding as in panel A was used, with two pK_a values (<6.2 and ~8.9) for Cyt*c*O in a detergent solution (black dots and line) and one pK_a of 7.3 for Cyt*c*O in vesicles (green squares and line). (C) For the N139D Cyt*c*O, the $P^3 \rightarrow F^3$ rates were determined from 580 nm and the fits yielded pK_a values of >10.8 and ~10.2 for the mutant Cyt*c*O in a detergent solution (black dots) and in vesicles (green squares), respectively. The data with detergent-solubilized Cyt*c*O are from refs 32 and 41. Experimental conditions were as described in the legend of Figure 2.

these kinetic phases display the same signs at 830 nm (increase in absorbance), it is easier to extract the rates at this wavelength than at 580 nm. With the detergent-solubilized Cyt*c*O at pH 7.4, two kinetic phases were observed with time constants of ~90 μs (~50% oxidation of Cu_A during the $P^3 \rightarrow F^3$ reaction) and 1.5 ms (oxidation of Cu_A during the $F^3 \rightarrow O^4$ reaction). At pH 7.4–7.5 and 9.4–9.5 the $P^3 \rightarrow F^3$ reaction was significantly slower with the membrane reconstituted ($\tau \cong 240$ μs and 1 ms, respectively) than with detergent-solubilized Cyt*c*O ($\tau \cong 90$ and 210 μs, respectively). The data in Figure 2B also show that the rate of the $P^3 \rightarrow F^3$ reaction at pH 7.5 in membrane-reconstituted Cyt*c*O was significantly slower than that at pH 6.5; i.e., with the membrane-reconstituted Cyt*c*O, there was a significant pH dependence in the rate in this pH region. At pH 10.0–10.4, the rates with detergent-solubilized and membrane-reconstituted Cyt*c*O were similar. Figure 3A shows the $P^3 \rightarrow F^3$ rate as a function of pH for the detergent-solubilized[32] and membrane-reconstituted Cyt*c*O. As seen in this figure, the decrease in this rate occurred at lower pH values with the membrane-reconstituted than with detergent-solubilized Cyt*c*O. A pK_a of 6.8 was determined for the membrane-reconstituted Cyt*c*O, assuming that the maximal rate at low pH was the same for the membrane-reconstituted and detergent-solubilized Cyt*c*Os.

Results from earlier studies have shown that the $F^3 \rightarrow O^4$ reaction in detergent solution displays two pK_a values of <6.4

dx.doi.org/10.1021/bi201795c | *Biochemistry* 2012, 51, 1092–1100

and 8.9.[4] Upon reconstitution into a membrane, the higher pK_a was not observed and the rate titrated with a pK_a of ≤7.3 (Figure 3B). This behavior is interpreted in terms of a lowering of the high-pK_a titration so that it merges with the lower-pK_a titration.

Because with the membrane-reconstituted Cyt*c*O the pK_a in the pH dependence of the $P^3 \rightarrow F^3$ reaction was shifted such that the maximal value at low pH could not be obtained, we repeated the experiments with a mutant Cyt*c*O (N139D) in which the pK_a of its pH dependence is shifted from 9.4 (in wild-type Cyt*c*O) to >11 in a detergent solution. As seen in Figure 3C, upon membrane reconstitution of the N139D mutant Cyt*c*O, the maximal rates at low pH were slightly higher than with the detergent-solubilized Cyt*c*O and the pK_a was slightly lowered to ∼10.2.

We also investigated the reaction of reduced Cyt*c*O with O_2 in membranes composed of only the zwitterionic DOPC or anionic DOPG (Figure 4) at pH 7.5. As seen in Figure 4A, with DOPC there was an increase in absorbance at 580 nm in the time range of 0−0.2 ms, associated with the $P^3 \rightarrow F^3$ reaction, comparable to that observed with detergent-solubilized Cyt*c*O. For vesicles composed of only DOPG, the $P^3 \rightarrow F^3$ absorbance change could not be resolved. A qualitatively intermediate behavior was observed with the soybean lipids. The $P^3 \rightarrow F^3$ rates with DOPG and DOPC were determined from the data at 830 nm (Figure 4B) and found to be approximately the same for the $P^3 \rightarrow F^3$ and $F^3 \rightarrow O^4$ reactions: 170 ± 50 μs and 1.9 ± 0.3 ms with DOPC, 200 ± 60 μs and 1.9 ± 0.3 ms with DOPG, and 190 ± 50 μs and 2.2 ± 0.4 ms with soybean lipids, respectively. Consequently, differences in rates between the different lipid compositions could not account for the differences in the shapes of the absorbance changes observed at 580 nm. The absorbance change at 580 nm contains contributions from both the $P^3 \rightarrow F^3$ reaction itself and also reduction of heme *a* (Cu_A to heme *a* electron transfer). Thus, also a change in the Cu_A−heme *a* equilibrium constant may result in changes in the shape of the absorbance changes. To determine whether the Cu_A−heme *a* equilibrium differed with the different lipid compositions, we determined the relative contribution of the $P^3 \rightarrow F^3$ kinetic phases at 830 nm (Figure 4B). With DOPC and DOPG, this contribution was 64 ± 4 and 41 ± 4%, respectively, of the total absorbance change at 830 nm (Figure 4C). As seen in Figure 4C, with the soybean lipids, the fraction $P^3 \rightarrow F^3$ absorbance change at 830 nm was intermediate between those observed with DOPC and DOPG (54 ± 2%).

As a comparison, we investigated the effect of membrane reconstitution (in nanodiscs; see ref 23 for a detailed description) on the O_2 reduction reaction in the ba_3 oxidase from *T. thermophilus*. This enzyme presumably uses only a single proton-uptake pathway both during reduction of the enzyme and during oxidation, after binding of O_2 to the reduced ba_3 oxidase.[33] This pathway overlaps in space with the K pathway in the *R. sphaeroides* Cyt*c*O, and it is thus termed a K pathway analogue. At pH 7.5, we observed an acceleration in the first proton-uptake phase from ∼1.0×10^4 to ∼2×10^4 s^{-1} upon reconstitution of the Cyt*c*O into a membrane (Figure 5A). The second proton uptake displayed approximately the same rate in a detergent solution as in the membrane. In addition, we observed a shift in the Cu_A−heme *b* equilibrium such that less heme *b* was reduced in the membrane environment (Figure 5B).

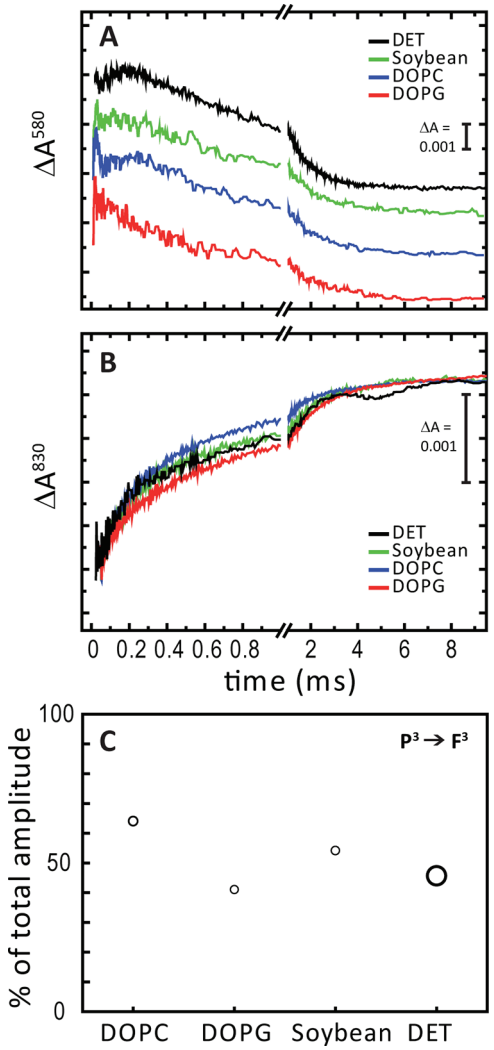

Figure 4. Absorbance changes during the O_2 reduction reaction at 580 (A) and 830 nm (B) in wild-type Cyt*c*O either in a detergent solution (black) or reconstituted into vesicles composed of soybean (green), zwitterionic DOPC (blue), or anionic DOPG (red) lipids. All traces were scaled to 1 μM reacting enzyme. For the experiments, vesicles containing 100 mM KCl, 25 mM HEPES (pH 7.5), and 100 μM EDTA on both sides of the membrane were mixed in a 1:1 ratio with an oxygen-saturated buffer with the same composition. For the detergent-solubilized samples, DDM at a concentration of 0.05% was added. (C) Fraction of the total amplitude of the absorbance increase at 830 nm, associated with the transfer of an electron from Cu_A to heme *a* (during the $P^3 \rightarrow F^3$ reaction). In vesicles composed of DOPC and DOPG, this fraction was 64 ± 4 and 41 ± 4%, respectively, while in soybean lipids as well as in a detergent solution, the fraction was intermediate between those observed with DOPC and DOPG, with values of 54 ± 2 and 46 ± 2% in soybean vesicles and a detergent solution, respectively. The size of the circles corresponds to the electron-transfer rate, where the smaller ones correspond to rate constants in the range of 5.0−5.9 × 10^3 s^{-1} (τ = 170−200 μs), while the larger circle (in DDM) corresponds to a rate constant of 1.1 × 10^4 s^{-1} (τ = 90 μs).

DISCUSSION

In this study, we determined the rate of the $P^3 \rightarrow F^3$ reaction in membrane-reconstituted Cyt*c*O at different pH values. At 580 nm, the increase in absorbance [most clearly seen with detergent-solubilized Cyt*c*O (Figure 2A, black traces)] reflects both formation of the F^3 state itself and a contribution from the

dx.doi.org/10.1021/bi201795c | *Biochemistry* 2012, 51, 1092−1100

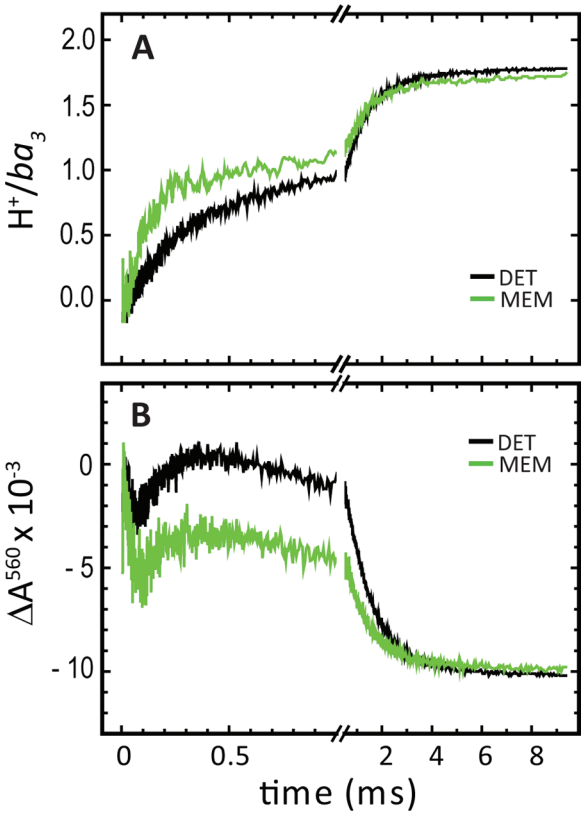

Figure 5. Absorbance changes associated with proton uptake (A) and the redox reaction of heme *b* (B) upon reaction of fully reduced cytochrome ba_3 with O_2. Black and green traces were obtained with CytcO in a detergent solution and reconstituted into a membrane using the nanodisc technology (for the reconstitution procedure, see ref 23), respectively. (A) Uptake of protons from solution was measured with the pH-sensitive dye phenol red, and the absorbance changes at 570 nm (converted to H^+/ba_3 enzyme) were followed, where an increase in absorbance is equivalent to the uptake of protons from solution. (B) Absorbance changes followed at 560 nm, where mainly redox reactions of heme *b* are observed (a decrease or increase in absorbance is associated with oxidation or reduction of the heme, respectively). Experimental conditions after mixing were as follows: pH 7.5 and ~22 °C with (A) 150 mM KCl and 40 μM phenol red or (B) 100 mM HEPES-KOH. In the detergent-solubilized sample, additional 0.05% DDM was present. The CO ligand was dissociated by a laser flash at time zero. Amplitudes are normalized to 1 μM reacting ba_3.

reduction of heme *a*. At 830 nm, the absorbance changes reflect oxidation of Cu_A, i.e., Cu_A–heme *a* electron transfer (Figure 2B). This transfer of an electron from Cu_A to heme *a* occurs over the same time scale as the $P^3 \rightarrow F^3$ reaction at the catalytic site, but the two reactions are independent.[34] As seen in Figure 4, differences were observed for the Cu_A–heme *a* equilibrium constant in DOPC or DOPG vesicles where during the $P^3 \rightarrow F^3$ reaction, 64 ± 4 and 41 ± 4%, respectively, of Cu_A was oxidized. The decrease in the fraction of oxidized Cu_A when the lipid is changed from the zwitterionic DOPC to the anionic DOPG cannot be due to electrostatic interactions between the lipid headgroups and Cu_A because an opposite behavior would be expected from an increase in the negative charge at the surface. The Cu_A site is located >15 Å from the protein–membrane interface, and electrostatic interactions near the protein–water interface are expected to be weak. Alternatively, the change in surface charge may alter the electrostatic field within the membrane-spanning part of the protein such that the heme *a* midpoint potential would decrease upon introduction of negative charge at the surface. To explain the difference in the Cu_A–heme *a* equilibrium constant, a difference of ~30 mV is required, which is relatively modest.

The major effect of membrane reconstitution on CytcO function was a decrease in the rate of the $P^3 \rightarrow F^3$ reaction at neutral pH. This effect was independent of lipid composition for soybean lipids, DOPG, and DOPC at neutral pH. On the basis of experiments with CytcO reconstituted in soybean lipids, the lower rate at neutral pH can be explained in terms of a lower pK_a value in the pH dependence of the rate of the $P^3 \rightarrow F^3$ reaction. The actual rate of the $P^3 \rightarrow F^3$ reaction (cf. proton-transfer rate) approaches the same value as in detergent solution at low pH (Figure 3). Earlier studies of the pH dependence of the $P^3 \rightarrow F^3$ transition indicate that transfer of a proton from solution, through the D pathway, to the catalytic site proceeds in two steps. First, a proton is transferred from Glu286 to the catalytic site with a time constant of ~90 μs, and then the Glu286 is rapidly ($\ll$90 μs) reprotonated from solution.[32] According to this model, Glu286 is in rapid ($\ll$90 μs) equilibrium with the bulk solution and the overall proton-uptake rate is determined by the fraction of protonated Glu286 (α_{EH}) multiplied by the rate of transfer of a proton from Glu286 to the catalytic site, k_H (1.1×10^4 s^{-1}; $\tau \cong 90$ μs)[32]

$$k_{PF} = \alpha_{EH} k_H = \frac{k_H}{1 + 10^{pH - pK_{E286}}} \quad (1)$$

where pK_{E286} is the pK_a of Glu286 (9.4) (see also Figure 3A). We note that an alternative model was suggested recently,[35] but that model would imply a high pK_a for the surface-exposed Asp132 (for CytcO in detergent solution), which we find highly unlikely.

Results from studies of different mutant CytcOs in which single-site amino acid residue replacements were made in the D pathway showed that the pK_a of Glu286 may be altered by several units (reviewed in ref 36). The pK_a both inicreased and decreased from the value in wild-type CytcO of 9.4,[32] and pK_a changes were observed also in cases where the net charge of the modified residue was unaltered.[5,36−42] To explain these observations, we previously extended the model outlined above to include two positions of the Glu286 side chain, E_1 and E_2, with different pK_a values, pK_{a1} and pK_{a2}, respectively.[36,43,44] The transfer of a proton to the catalytic site would occur only from one of these positions, E_2. Depending on the equilibrium constant between states E_1 and E_2, any apparent Glu286 pK_a value in the range between pK_{a1} and pK_{a2} would be observed even if the pK_a values were fixed.[36,43] To explain changes in the apparent Glu286 pK_a as a result of the structural alterations within the D pathway discussed above, we proposed that these alterations modulate the Glu286 equilibrium, thereby stabilizing one of the E states relative to the other. Similarly, introduction of a membrane around the CytcO may result in changes in the E_1–E_2 equilibrium constant. When considering the specific parameters used in refs 36 and 43, the membrane would stabilize state E_1 relative to state E_2. However, introduction of a membrane may result not only in alteration of the equilibrium constant between the two E states but also in alteration of the pK_a values of Glu286 in these states (i.e., pK_{a1} and pK_{a2}), which makes it difficult to present any quantitative analysis here. Such an analysis could be further complicated by a possible contribution of Asp132 to the pH dependence profile

dx.doi.org/10.1021/bi201795c | *Biochemistry* 2012, 51, 1092−1100

because this residue may have a pK_a[45] in the region where the rate of the $P^3 \rightarrow F^3$ reaction titrates in the presence of a membrane (Figure 3). Nonetheless, we consider changes in the equilibrium constant between the two E states to significantly contribute to the pK_a shifts observed here because such changes are qualitatively supported by results from a recent theoretical study.[46]

Because with the membrane-reconstituted wild-type CytcO we could not observe a maximal saturation rate at low pH values, we repeated the experiments discussed above with the N139D mutant CytcO in which the pK_a in the $P^3 \rightarrow F^3$ pH dependence is shifted from 9.4 to >11.[41] We reasoned that with this elevated pK_a value we would be able to compare the maximal proton-uptake rates at low pH in detergent solution and in SUVs. As seen in Figure 3C, the maximal rates in the low-pH range were slightly accelerated upon reconstitution of the CytcO into SUVs. Furthermore, the pK_a decreased from >11 to ~10.2. In the framework of the model described above (see eq 1), these results indicate that, upon membrane reconstitution, the rate of internal transfer of a proton from Glu286 to the catalytic site is somewhat accelerated. The small increase in the rate may be explained in terms of changes in the structure or electrostatic field around the Glu286 upon membrane reconstitution (see below). The lowering of the Glu286 pK_a upon membrane reconstitution was qualitatively similar to the results with wild-type CytcO. However, this effect was smaller presumably because the effect of the N139D mutation dominates over the effect of membrane reconstitution.

The effect of membrane reconstitution on the pH dependence of the $F^3 \rightarrow O^4$ reaction is more complicated than for the $P^3 \rightarrow F^3$ reaction.[47] This is presumably because, in contrast to the latter reaction, the former involves the transfer of an electron to the catalytic site in addition to the transfer of a proton. Earlier analyses of the pH dependence of this reaction showed that the protonation state of two protonatable groups determines the rate of the $F^3 \rightarrow O^4$ reaction . One group is Glu286, which affects the proton-transfer rate as it does for the $P^3 \rightarrow F^3$ reaction ($pK_a \sim 9$). The second group is located around the heme a_3 D-ring propionate, and its protonation state determines the electron equilibrium within the enzyme, which determines the reduction rate of the catalytic site.[47] As seen in Figure 3B, the high-pH titration was not observed with the membrane-reconstituted CytcO. Instead, a titration in the pH range of <8 was observed, which is consistent with the lowering of the pK_a for the $P^3 \rightarrow F^3$ reaction. The low-pK_a titration in detergent solution either may be shifted to lower pH values outside of the accessible pH range upon membrane reconstitution or may overlap with the observed high-pH titration (that is lowered upon membrane reconstitution).

In general, slower turnover rates are observed upon reconstitution of CytcO into lipid vesicles at neutral pH (see, for example, refs 48 and 49), which is qualitatively consistent with the data from this study. However, data from turnover experiments cannot be directly compared to the results from measurements of specific reaction rates because events other than those studied here may be rate-limiting for the CytcO turnover.

Results from studies of the proton-transfer kinetics through the K pathway in the absence of O_2 showed that the rate increased by a factor of almost 10 upon membrane reconstitution.[21,22] In that study, the effect was attributed to specific interactions between lipid headgroups and an acidic residue near the orifice of the K pathway.[22] This site is located close to the protein−membrane interface,[50,51] and therefore, such interactions are likely to be significant. In this study, we investigated reactions linked to proton uptake through the D pathway, which has its orifice >10 Å from the protein−membrane interface. Consequently, interactions with the lipid headgroups are less likely, and the observed effects are expected to originate from changes in the internal electrostatic field and/or membrane stabilization of specific structural substates (cf. stabilization of a specific configuration of an amino-acid residue side chain[46]).

For comparison, we also studied the reaction with O_2 of the reduced ba_3 CytcO from *T. thermophilus*, which uses the single K pathway analogue for all proton-uptake reactions. In the ba_3 CytcO, the rate of the first proton-uptake reaction through the K pathway analogue was a factor of 2 faster in the membrane-reconstituted CytcO than in detergent solution, which is opposite of the effect observed for the CytcO oxidation of the aa_3 *R. sphaeroides* oxidase (see Figure 5). On the other hand, the acceleration in rate upon ba_3 CytcO membrane reconstitution is consistent with the results for the transfer of a proton through the K pathway in the aa_3 CytcO in a different experiment.[22] Thus, these data further confirm that the slowed proton-uptake rate at neutral pH upon membrane reconstitution of the aa_3 CytcO is an effect that is attributed to changes around or in the D pathway.

The structure and function of membrane proteins are often dependent on specific interactions between membrane lipids and the protein. In many cases, lipids occupy specific binding sites within a protein and can be considered as structural (and functional) components of the protein (for reviews, see refs 15 and 17−19). For example, a comparison of CytcOs from different organisms showed that lipids and detergents occupy highly conserved binding sites,[10,15] and replacement of these lipids may modulate the CytcO function.[20] Furthermore, the surrounding membrane can influence the function of a reconstituted enzyme, for example, by altering the electrostatic environment or by stabilizing specific structural states. In CytcO, functionally relevant structural changes have been observed; however, these changes primarily involve specific amino acid residues or movement of helices,[52−56] and most likely they do not extend toward the enzyme surface. Consequently, as already mentioned above, the effect on the pH dependence profile of the $P^3 \rightarrow F^3$ and $F^3 \rightarrow O^4$ reactions most likely originates from changes in the electrostatic field within the CytcO upon membrane reconstitution.

Summary. Earlier results from studies of the transfer of a proton through the K pathway, which begins near the CytcO−membrane interface, showed that this rate is accelerated upon incorporation of the CytcO into a membrane. This effect was explained in terms of extension of the proton-collecting surface area around the orifice of the proton pathway. In contrast, the maximal proton-uptake rate through the D pathway at low pH was only slightly accelerated upon membrane reconstitution (see Figure 3C). Qualitatively, the much smaller effect on the proton-uptake rate is consistent with the D pathway orifice being located >10 Å from the CytcO−membrane interface. When considering our model describing the uptake of a proton through the D pathway during O_2 reduction (see eq 1), the uptake of a proton by Glu286 is not rate-limiting, so that any acceleration in this rate would not be observed. The most significant effect of membrane reconstitution was a lowering of the pK_a in the pH dependence of the proton-uptake rate, which

results in slower proton uptake at neutral pH. We propose that this effect is due to changes in the environment of the CytcO such that the dynamics and structural equilibrium[46] of the Glu286 side chain changes result in a lowering of the apparent pK_a associated with the proton-transfer reaction.

In general, the data from this study show that there are significant functional differences between the detergent-solubilized and membrane-reconstituted CytcO. The latter is presumably a better mimic of the native system, although the membrane curvature and the lipid:protein ratio are larger in the SUVs than in the cell. Furthermore, in our experiments, there is no transmembrane electrochemical proton gradient. Nevertheless, the results show that the kinetic and thermodynamic parameters of the studied CytcO reactions are affected by the lipid environment.

AUTHOR INFORMATION

Corresponding Author

*E-mail: peterb@dbb.su.se. Fax: +46-8-153679. Phone: +46 8 16 32 80.

Funding

These studies were supported by grants from the Swedish Research Council. C.v.B. is supported by a fellowship from the Swiss National Science Foundation (SNF).

Notes

The authors declare no competing financial interest.

ABBREVIATIONS

CytcO, cytochrome *c* oxidase; *n* side, negative side of the membrane; *p* side, positive side of the membrane; SU, subunit time constants as (rate constant)$^{-1}$; DDM, *n*-dodecyl β-D-maltoside; DOPG, 1,2-dioleoyl-*sn*-glycero-3-phospho(1-*rac*-glycerol); DOPC, 1,2-dioleoyl-*sn*-glycero-3-phosphocholine. If not otherwise indicated, amino acid residues are numbered according to the *R. sphaeroides* CytcO sequence and the residues are found in subunit I.

REFERENCES

(1) Hosler, J. P., Ferguson-Miller, S., and Mills, D. A. (2006) Energy transduction: Proton transfer through the respiratory complexes. *Annu. Rev. Biochem. 75*, 165−187.

(2) Yoshikawa, S., Muramoto, K., Shinzawa-Itoh, K., Aoyama, H., Tsukihara, T., Shimokata, K., Katayama, Y., and Shimada, H. (2006) Proton pumping mechanism of bovine heart cytochrome c oxidase. *Biochim. Biophys. Acta 1757*, 1110−1116.

(3) Wikström, M., and Verkhovsky, M. I. (2006) Towards the mechanism of proton pumping by the haem-copper oxidases. *Biochim. Biophys. Acta 1757*, 1047−1051.

(4) Namslauer, A., and Brzezinski, P. (2004) Structural elements involved in electron-coupled proton transfer in cytochrome c oxidase. *FEBS Lett. 567*, 103−110.

(5) Brzezinski, P., and Gennis, R. B. (2008) Cytochrome c oxidase: Exciting progress and remaining mysteries. *J. Bioenerg. Biomembr. 40*, 521−531.

(6) Brzezinski, P., and Ädelroth, P. (2006) Design principles of proton-pumping haem-copper oxidases. *Curr. Opin. Struct. Biol. 16*, 465−472.

(7) Richter, O. M. H., and Ludwig, B. (2009) Electron transfer and energy transduction in the terminal part of the respiratory chain: Lessons from bacterial model systems. *Biochim. Biophys. Acta 1787*, 626−634.

(8) Belevich, I., and Verkhovsky, M. I. (2008) Molecular mechanism of proton translocation by cytochrome c oxidase. *Antioxid. Redox Signaling 10*, 1−29.

(9) Svensson-Ek, M., Abramson, J., Larsson, G., Törnroth, S., Brzezinski, P., and Iwata, S. (2002) The X-ray Crystal Structures of Wild-Type and EQ(I-286) Mutant Cytochrome *c* Oxidases from *Rhodobacter sphaeroides*. *J. Mol. Biol. 321*, 329−339.

(10) Qin, L., Hiser, C., Mulichak, A., Garavito, R. M., and Ferguson-Miller, S. (2006) Identification of conserved lipid/detergent-binding sites in a high-resolution structure of the membrane protein cytochrome c oxidase. *Proc. Natl. Acad. Sci. U.S.A. 103*, 16117−16122.

(11) Montecucco, C., Smith, G. A., Dabbeni-sala, F., Johannsson, A., Galante, Y. M., and Bisson, R. (1982) Bilayer thickness and enzymatic activity in the mitochondrial cytochrome c oxidase and ATPase complex. *FEBS Lett. 144*, 145−148.

(12) Zhang, X., Tamot, B., Hiser, C., Reid, G. E., Benning, C., and Ferguson-Miller, S. (2011) Cardiolipin Deficiency in *Rhodobacter sphaeroides* Alters the Lipid Profile of Membranes and of Crystallized Cytochrome Oxidase, but Structure and Function Are Maintained. *Biochemistry 50*, 3879−3890.

(13) Zhang, X., Hiser, C., Tamot, B., Benning, C., Reid, G. E., and Ferguson-Miller, S. M. (2011) Combined genetic and metabolic manipulation of lipids in *Rhodobacter sphaeroides* reveals non-phospholipid substitutions in fully active cytochrome c oxidase. *Biochemistry 50*, 3891−3902.

(14) Liu, J., Qin, L., and Ferguson-Miller, S. (2011) Crystallographic and online spectral evidence for role of conformational change and conserved water in cytochrome oxidase proton pump. *Proc. Natl. Acad. Sci. U.S.A. 108*, 1284−1289.

(15) Qin, L., Sharpe, M. A., Garavito, R. M., and Ferguson-Miller, S. (2007) Conserved lipid-binding sites in membrane proteins: A focus on cytochrome c oxidase. *Curr. Opin. Struct. Biol. 17*, 444−450.

(16) Qin, L., Mills, D. A., Buhrow, L., Hiser, C., and Ferguson-Miller, S. (2008) A conserved steroid binding site in cytochrome c oxidase. *Biochemistry 47*, 9931−9933.

(17) Lee, A. G. (2004) How lipids affect the activities of integral membrane proteins. *Biochim. Biophys. Acta 1666*, 62−87.

(18) Lee, A. G. (2011) Lipid-protein interactions. *Biochem. Soc. Trans. 39*, 761−766.

(19) Hunte, C., and Richers, S. (2008) Lipids and membrane protein structures. *Curr. Opin. Struct. Biol. 18*, 406−411.

(20) Varanasi, L., Mills, D., Murphree, A., Gray, J., Purser, C., Baker, R., and Hosler, J. (2006) Altering conserved lipid binding sites in cytochrome c oxidase of *Rhodobacter sphaeroides* perturbs the interaction between subunits I and III and promotes suicide inactivation of the enzyme. *Biochemistry 45*, 14896−14907.

(21) Belevich, I., Tuukkanen, A., Wikström, M., and Verkhovsky, M. I. (2006) Proton-coupled electron equilibrium in soluble and membrane-bound cytochrome c oxidase from *Paracoccus denitrificans*. *Biochemistry 45*, 4000−4006.

(22) Näsvik Öjemyr, L., Lee, H. J., Gennis, R. B., and Brzezinski, P. (2010) Functional interactions between membrane-bound transporters and membranes. *Proc. Natl. Acad. Sci. U.S.A. 107*, 15763−15767.

(23) Näsvik Öjemyr, L., von Ballmoos, C., Gennis, R. B., Sligar, S. G., and Brzezinski, P. (2011) Reconstitution of Respiratory Oxidases in Membrane Nanodiscs for Investigation of Proton-Coupled Electron Transfer. *FEBS Lett.*, doi: 10.1016/j.febslet.2011.12.023.

(24) Brändén, G., Gennis, R. B., and Brzezinski, P. (2006) Transmembrane proton translocation by cytochrome *c* oxidase. *Biochim. Biophys. Acta 1757*, 1052−1063.

(25) Mitchell, D. M., and Gennis, R. B. (1995) Rapid purification of wildtype and mutant cytochrome c oxidase from *Rhodobacter sphaeroides* by Ni^{2+}-NTA affinity chromatography. *FEBS Lett. 368*, 148−150.

(26) Smirnova, I., Reimann, J., Von Ballmoos, C., Chang, H. Y., Gennis, R. B., Fee, J. A., Brzezinski, P., and Ädelroth, P. (2010) Functional role of Thr-312 and Thr-315 in the proton-transfer pathway in ba_3 cytochrome *c* oxidase from *Thermus thermophilus*. *Biochemistry 49*, 7033−7039.

(27) Wiedenmann, A., Dimroth, P., and Von Ballmoos, C. (2009) Functional asymmetry of the F0 motor in bacterial ATP synthases. *Mol. Microbiol. 72*, 479−490.
(28) Faxén, K., and Brzezinski, P. (2007) The inside pH determines rates of electron and proton transfer in vesicle-reconstituted cytochrome c oxidase. *Biochim. Biophys. Acta 1767*, 381−386.
(29) Jasaitis, A., Verkhovsky, M. I., Morgan, J. E., Verkhovskaya, M. L., and Wikström, M. (1999) Assignment and charge translocation stoichiometries of the major electrogenic phases in the reaction of cytochrome c oxidase with dioxygen. *Biochemistry 38*, 2697−2706.
(30) Faxén, K., Gilderson, G., Ädelroth, P., and Brzezinski, P. (2005) A mechanistic principle for proton pumping by cytochrome c oxidase. *Nature 437*, 286−289.
(31) Brändén, M., Sigurdson, H., Namslauer, A., Gennis, R. B., Ädelroth, P., and Brzezinski, P. (2001) On the role of the K-proton transfer pathway in cytochrome c oxidase. *Proc. Natl. Acad. Sci. U.S.A. 98*, 5013−5018.
(32) Namslauer, A., Aagaard, A., Katsonouri, A., and Brzezinski, P. (2003) Intramolecular proton-transfer reactions in a membrane-bound proton pump: The effect of pH on the peroxy to ferryl transition in cytochrome c oxidase. *Biochemsitry 42*, 1488−1498.
(33) Chang, H. Y., Hemp, J., Chen, Y., Fee, J. A., and Gennis, R. B. (2009) The cytochrome ba_3 oxygen reductase from *Thermus thermophilus* uses a single input channel for proton delivery to the active site and for proton pumping. *Proc. Natl. Acad. Sci. U.S.A. 106*, 16169−16173.
(34) Karpefors, M., Ädelroth, P., Zhen, Y., Ferguson-Miller, S., and Brzezinski, P. (1998) Proton uptake controls electron transfer in cytochrome c oxidase. *Proc. Natl. Acad. Sci. U.S.A. 95*, 13606−13611.
(35) Wikström, M., and Verkhovsky, M. I. (2011) The D-channel of cytochrome oxidase: An alternative view. *Biochim. Biophys. Acta 1807*, 1273−1278.
(36) Brzezinski, P., and Johansson, A. L. (2010) Variable proton-pumping stoichiometry in structural variants of cytochrome c oxidase. *Biochim. Biophys. Acta 1797*, 710−723.
(37) Namslauer, I., Lee, H. J., Gennis, R. B., and Brzezinski, P. (2010) A pathogenic mutation in cytochrome c oxidase results in impaired proton pumping while retaining O_2-reduction activity. *Biochim. Biophys. Acta 1797*, 550−556.
(38) Lepp, H., Salomonsson, L., Zhu, J. P., Gennis, R. B., and Brzezinski, P. (2008) Impaired proton pumping in cytochrome c oxidase upon structural alteration of the D pathway. *Biochim. Biophys. Acta 1777*, 897−903.
(39) Han, D., Namslauer, A., Pawate, A., Morgan, J. E., Nagy, S., Vakkasoglu, A. S., Brzezinski, P., and Gennis, R. B. (2006) Replacing Asn207 by Aspartate at the Neck of the D Channel in the aa_3-Type Cytochrome c Oxidase from *Rhodobacter sphaeroides* Results in Decoupling the Proton Pump. *Biochemistry 45*, 14064−14074.
(40) Brändén, G., Pawate, A. S., Gennis, R. B., and Brzezinski, P. (2006) Controlled uncoupling and recoupling of proton pumping in cytochrome *c* oxidase. *Proc. Natl. Acad. Sci. U.S.A. 103*, 317−322.
(41) Namslauer, A., Pawate, A. S., Gennis, R. B., and Brzezinski, P. (2003) Redox-coupled proton translocation in biological systems: Proton shuttling in cytochrome c oxidase. *Proc. Natl. Acad. Sci. U.S.A. 100*, 15543−15547.
(42) Namslauer, A., Lepp, H., Brändén, M., Jasaitis, A., Verkhovsky, M. I., and Brzezinski, P. (2007) Plasticity of proton pathway structure and water coordination in cytochrome c oxidase. *J. Biol. Chem. 282*, 15148−15158.
(43) Chakrabarty, S., Namslauer, I., Brzezinski, P., and Warshel, A. (2011) Exploration of the cytochrome c oxidase pathway puzzle and examination of the origin of elusive mutational effects. *Biochim. Biophys. Acta 1807*, 413−426.
(44) Johansson, A. L., Chakrabarty, S., Berthold, C. L., Högbom, M., Warshel, A., and Brzezinski, P. (2011) Proton-transport mechanisms in cytochrome c oxidase revealed by studies of kinetic isotope effects. *Biochim. Biophys. Acta 1807*, 1083−1094.
(45) Ädelroth, P., and Hosler, J. (2006) Surface proton donors for the D-pathway of cytochrome c oxidase in the absence of subunit III. *Biochemistry 45*, 8308−8318.
(46) Yang, S., and Cui, Q. (2011) Glu286 rotation and water wire reorientation are unlikely the gating elements for proton pumping in cytochrome *c* oxidase. *Biophys. J. 101*, 61−69.
(47) Brändén, G., Brändén, M., Schmidt, B., Mills, D. A., Ferguson-Miller, S., and Brzezinski, P. (2005) The protonation state of a heme propionate controls electron transfer in cytochrome c oxidase. *Biochemistry 44*, 10466−10474.
(48) Cvetkov, T. L., and Prochaska, L. J. (2007) Biophysical and biochemical characterization of reconstituted and purified *Rhodobacter sphaeroides* cytochrome c oxidase in phospholipid vesicles sheds insight into its functional oligomeric structure. *Protein Expression Purif. 56*, 189−196.
(49) Mills, D. A., and Ferguson-Miller, S. (2002) Influence of structure, pH and membrane potential on proton movement in cytochrome oxidase. *Biochim. Biophys. Acta 1555*, 96−100.
(50) Brändén, M., Tomson, F., Gennis, R. B., and Brzezinski, P. (2002) The entry point of the K-proton-transfer pathway in cytochrome c oxidase. *Biochemistry 41*, 10794−10798.
(51) Tomson, F. L., Morgan, J. E., Gu, G., Barquera, B., Vygodina, T. V., and Gennis, R. B. (2003) Substitutions for glutamate 101 in subunit II of cytochrome c oxidase from *Rhodobacter sphaeroides* result in blocking the proton-conducting K-channel. *Biochemistry 42*, 1711−1717.
(52) Qin, L., Liu, J., Mills, D. A., Proshlyakov, D. A., Hiser, C., and Ferguson-Miller, S. (2009) Redox-dependent conformational changes in cytochrome c oxidase suggest a gating mechanism for proton uptake. *Biochemistry 48*, 5121−5130.
(53) Muramoto, K., Ohta, K., Shinzawa-Itoh, K., Kanda, K., Taniguchi, M., Nabekura, H., Yamashita, E., Tsukihara, T., and Yoshikawa, S. (2010) Bovine cytochrome c oxidase structures enable O_2 reduction with minimization of reactive oxygens and provide a proton-pumping gate. *Proc. Natl. Acad. Sci. U.S.A. 107*, 7740−7745.
(54) Muramoto, K., Hirata, K., Shinzawa-Itoh, K., Yoko-o, S., Yamashita, E., Aoyama, H., Tsukihara, T., and Yoshikawa, S. (2007) A histidine residue acting as a controlling site for dioxygen reduction and proton pumping by cytochrome c oxidase. *Proc. Natl. Acad. Sci. U.S.A. 104*, 7881−7886.
(55) Busenlehner, L. S., Salomonsson, L., Brzezinski, P., and Armstrong, R. N. (2006) Mapping protein dynamics in catalytic intermediates of the redox-driven proton pump cytochrome c oxidase. *Proc. Natl. Acad. Sci. U.S.A. 103*, 15398−15403.
(56) Busenlehner, L. S., Brändén, G., Namslauer, I., Brzezinski, P., and Armstrong, R. N. (2008) Structural elements involved in proton translocation by cytochrome c oxidase as revealed by backbone amide hydrogen-deuterium exchange of the E286H mutant. *Biochemistry 47*, 73−83.